결정립 조대화된 기계적 합금화 ODS NiAl의 Creep 성질

어 순 철 · 서 성 재*

충주산업대학교 재료공학과
* 쌍용중공업(주) 엔진기술연구소

Creep Properties of Grain Coarsened ODS MA NiAl

Soon-Chul Ur and Sung-Jae Suh*

Dept. of Materials Science and Engineering, Chung-Ju National University, Chung-Ju, 380-702
*Engine Research Institute, SSang-Yong Heavy Industries Co., Ltd., Chang Won, 641-315

초 록　NiAl기 산화물 분산강화(Oxide Dispersion Strengthened: ODS) 합금을 기계적 합금화 (Mechanical Alloying: MA) 방법으로 제조하였으며, 열간압축방법으로 성형하였다. 연이어 단순항온처리에 의한 정상결정립성장과 특정조건에서의 thermomechanical treatment에 의한 이차재결정화를 유도하였다. 결정립 조대화된 ODS MA NiAl의 creep 성질 및 이에 수반된 creep 기구를 조사하였으며, 여러 다른 미세조직과의 상관관계를 비교 분석하였다. 정상결정립성장기구에 의해 조대화된 미세조직은 creep 성질이 저하된 반면, 이차재결정화된 MA NiAl의 creep 성질은 크게 향상되었다. 이 creep 성질의 향상은 이차재결정화의 특성인 급격한 결정립의 조대화, 분산상의 성장억제 및 grain aspect ratio의 증가에 기인한 것으로 사료되었다. 이차재결정화된 ODS MA NiAl의 creep을 위한 겉보기 활성화에너지와 응력지수(stress exponent)의 범위는 본 실험조건에서는 주 creep기구가 climb controlled dislocation creep 또는 glide controlled dislocation creep임을 제시하지만, 전체 creep 속도가 결정립 크기 및 grain aspect ratio의 영향을 크게 받은 것을 볼 때, 결정립계 미끄럼기구가 주 creep 기구와 조합되어 MA NiAl의 전체 creep기구에 영향을 준 것으로 추정할 수 있었다.

Abstract　NiAl based oxide dispersion strengthened(ODS) intermetallic alloys have been produced by mechanical alloying(MA) and consolidated by hot extrusion. Subsequent isothermal annealing has been carried out to induce normal grain growth(NGG) and thermomechanical treatment under specific condition has been applied to induce secondary recrystallization(SRx). Creep properties of ODS MA NiAl have been investigated, and the associated creep mechanisms have been evaluated for the given condition. The creep properties of the grain coarsened MA NiAl have been also compared with those of as-consolidated MA NiAl and other counterparts. It has been shown that SRx leads to a pronounced grain coarsening and high grain aspect ratio without concurrent dispersoid coarsening, which results in improved creep resistance, whereas limited grain coarsening with dispersoid coarsening by NGG mechanism degrades creep resistance.

　The apparent activation energy and the stress exponent for creep in SRxed MA NiAl indicate that creep is controlled by one of the dislocation creep mechanisms, either climb controlled or viscous glide controlled. However, a grain size dependence on creep has been shown, indicating that grain boundary sliding mechanism accommodated by major creep mechanism contributes to the overall deformation in MA NiAl.

1. Introduction

Intermetallic compound NiAl with ordered B_2 structure has a great potential for high temperature applications because of its low density, high melting point, high thermal conductivity and excellent oxidation resistance[1]. However, cast, polycrystalline NiAl suffers from poor ambient temperature ductility and poor creep resistance at intended service temperature, which indicates that the use of monolithic material is improbable[1,2]. In an effort to address these problems an approach has been done to synthesize ODS NiAl by mechanical alloying of elemental Ni and Al powders.

It is well known that, at the highest service temperature, dispersion strengthening(DS) is superior to precipitate strengthening because dispersoids are not prone to dissolution and in general the coarsening rates are much slower than precipitates. This is clearly demonstrated by the performance of ODS superalloys such as MA6000[3]. The role of the dispersoids in high temperature creep is to act as significant obstacles to the motion of dislocations and prevent grain boundary sliding effectively, increasing the creep resistance in dislocation creep[3,4].

Table 1. Chemical compositions of as-milled MA NiAl powder

Element	Ni	Al	H	O	C	N	Fe	Ti
Atomic %	47.46	49.60	218 ppm	2.6	0.04	0.064	0.12	0.63

It is well established that there is a strong grain size dependence in diffusional creep while no apparent grain size effect is expected in the dislocation creep regime[4]. However, the grain boundary sliding accommodation process by either diffusion or dislocation creep mechanisms are always expected at high temperatures[3, 5]. Therefore, a larger grain size containing finely distributed dispersoids, which can be developed by secondary recrystallization mechanism, is generally preferred in creep resistant materials[6]. The high temperature strength of ODS materials can be further improved by producing a highly -elongated or fibrous grain microstructure aligned parallel to the stress axis, which reduces grain boundary sliding and minimizes transverse rupture by control of cavitation on transverse boundaries[7]. Such structures can be produced by secondary recrystallization mechanism and we have therefore undertaken thermomechanical treatments to promote SRx in MA NiAl to further improve its creep resistance[8].

In an attempt to produce another type of coarse grain structure, normal grain growth, in which grain growth and dispersoid coarsening are generally concurrent[8], have also been induced by isothermal annealing to characterize and compare creep mechanisms in MA NiAl.

In this article, results of recent studies on creep in grain coarsened MA NiAl materials are presented, discussed, and contrasted with the results of analogous studies of their as-consolidated conditions as well as conventionally processed counterparts.

2. Experimental Procedure

The dispersion strengthened NiAl powders are prepared by high energy ball milling a mixture of elemental Al and Ni powders using a modified Szegvari attrition mill in an argon atmosphere. The compositions of the as-milled powder is shown in Table 1.

The powder was sieved to -325 mesh after milling for 70 hrs, and consolidated by hot extrusion. Hot extruded(EX) bar was produced at 1127℃ with an extrusion ratio of 16 : 1 after degassing in vacuum at 800℃. Hot extruded specimens were isothermally annealed to produce NGG structure in a vacuum furnace at 1400℃ for an hour with a heating rate of 250 K/min and cooled to room temperature in air. Thermomechanical treatments utilizing prestrain and isothermal annealing

were carried out to induce SRx. The prestrain was introduced by uniaxial compression to 5% strain in a universal testing machine. Then the prestrained EX specimens were isothermally annealed above TSRx for 30 min, as specified previously[8]. Microstructures of grain coarsened specimens in both transverse and longitudinal sections were optically investigated for any changes of grain size as well as grain aspect ratio.

Compressive creep tests were performed utilizing a modified Satec M-3 creep testing machine. Constant load were applied ranging from 40 to 180MPa at 800℃, 850℃ and 900℃. For compressive creep tests, cylindrical specimens(5mmϕx 10mmL or 4mmϕx 8mmL) were machined from heat treated specimens parallel to the extrusion axis by electro-discharge machining(EDM). Before creep test, EDM cut specimens were inspected using a low magnification microscope to ensure microcrack free surfaces.

The creep strain curves as functions of time at a given temperature and stress were obtained. Steady state creep rate($\dot{\epsilon}_s$) was calculated using computerized linear regression method applied to the data in the time interval between 15 and 20 hours. Then an Arrhenius plot of ln $\dot{\epsilon}_s$ versus 1/T was made to obtain the apparent activation energy(Q_{app}) for creep. A plot of ln $\dot{\epsilon}_s$ versus ln σ for a given microstructure was also made in order to compare the creep behavior with as-consolidated specimens and other counterparts as well as to obtain the stress exponent(n).

Microstructures of crept specimens in both transverse and longitudinal sections were also optically investigated for any structural changes.

3. Results and discussion

The primary microstructures after consolidation are typically fine grained with a grain size less than 1 μm, and contain a fine distribution of Al_2O_3 dispersoids in the range of 10~100 nm[8, 9]. The microstructures after simple isothermal annealing at 1400℃ for an hour show typical normal grain growth, in which grain growth and dispersoid coarsening are generally concurrent, with a average grain size of 15μm[5]. A substantially SRxed microstructure was produced in the material homogeneously prestrained about 5% followed by isothermal annealing at 1300℃ for 30 min. Here, it was possible to have crack free prestrained specimens by

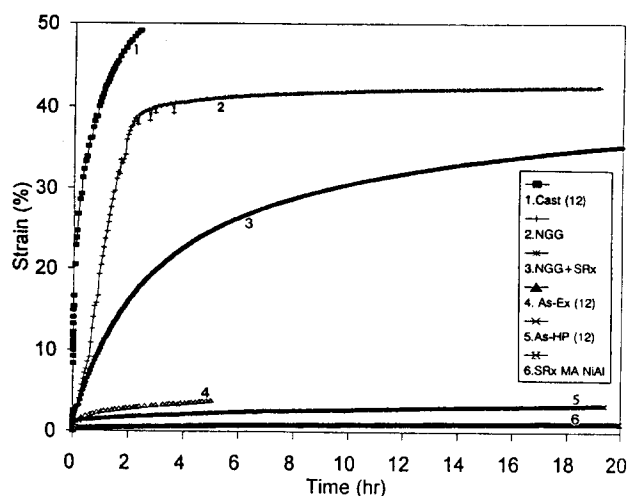Fig. 1. Optical micrographs of SRx MA NiAl, (a) transverse section (b) longitudinal Sction.

Fig. 2. General trends in creep curves of MA NiAl, at 110MPa and 850℃.

compression, since MA NiAl showed significantly improved compressive ductility at room temperature due to additional slip system operations, though it was still shown to have near zero tensile ductility as in other intermetallics[9]. It is shown that dispersoids remain fine during the process of SRx, since dispersoid coarsening is suppressed due to the grain boundary break-away process of SRx[8]. The microstructure of sections parallel to the extrusion axis typically consists of well developed elongated, SRxed grains having a grain aspect ratio of 5 (200~500μm × 1000~2000μm), as shown in Fig. 1. This type of elongated grain structure is commonly observed after isothermal annealing or zone annealing of ODS superalloys[3,6,7]. It has been suggested that this reflects either the alignment of the dispersoid along the extrusion axis restricting lateral growth or a texture effect which leads to lateral grain boundaries

being mobile than others[7].

General creep trends.

Compressive creep tests were performed on SRxed and NGG specimens applying a constant load parallel to the extrusion axis ranging from 40 MPa to 180 MPa at 800℃, 850℃ and 900℃ for 20 hours. The normalized creep conditions in this study are $0.56 \leq T/T_M \leq 0.61$ and $4 \times 10^{-4} \leq \sigma/G \leq 3 \times 10^{-3}$, assuming no significant differences in shear modulus between as-extruded and SRx conditions. Creep curves of grain coarsened specimens obtained at 850℃ and 110MPa are presented in Fig. 2. In the figure, creep curves of as-consolidated MA NiAl as well as single phase, cast NiAl, of which average grain size is 40μm, are presented for comparison. The creep curves show primary and steady state creep but not tertiary creep in this study, due to the compressive creep mode used, in which most microstructure instabilities such as microcracking or necking are suppressed[10].

As can be seen, the creep properties of ODS MA NiAl, in terms of creep strain, are considerably improved by SRx, while the curve of NGG specimen shows very poor creep resistance despite a large grain size in comparison with as-consolidated specimens. Significant dispersoid coarsening in the NGG specimen is responsible for the poor creep properties similar to the creep of single phase NiAl (curve 1 in the figure). On the other hand, the considerable increase in grain size combined with fine dispersoid size in the SRx specimens is responsible for the improved creep resistance. Partially SRxed specimens(SRx+NGG), which are occasionally produced during the thermomechanical treatments, show large creep strains and a high creep rate due to the poor creep properties of the NGG area in the specimen. When steady state creep rates or minimum creep rates ($\dot{\varepsilon}_s$) are considered in characterizing the creep properties, care must be taken since large creep strains lead to a reduction in an effective stress resulting in lower apparent creep rates in compression creep mode. Indeed, the estimated effective stress of the NGG specimen at the end of test is about 76MPa and the steady state creep rate appears to be comparable to that of SRxed specimens, as shown in Fig. 2. For the materials with low creep strains in the test condition (curves 4 to 6), creep strains are proportional to the steady state creep rates in this study.

Microstructure characterization of crept specimens.

The shapes of crept specimens, which were tested at 850℃ and 110MPa for 20 hours, are presented in Fig. 3. The initial size of the specimens was 4mm diameter
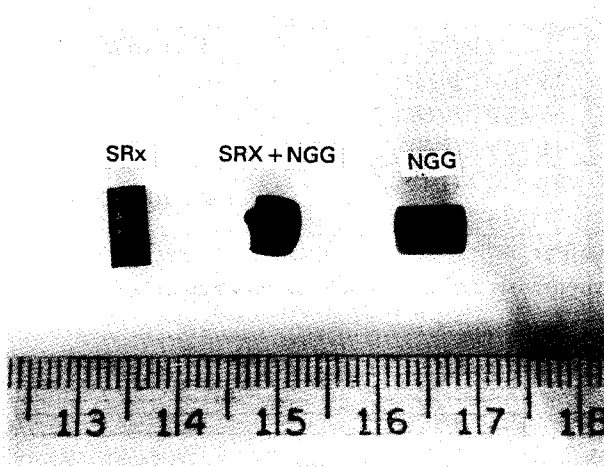
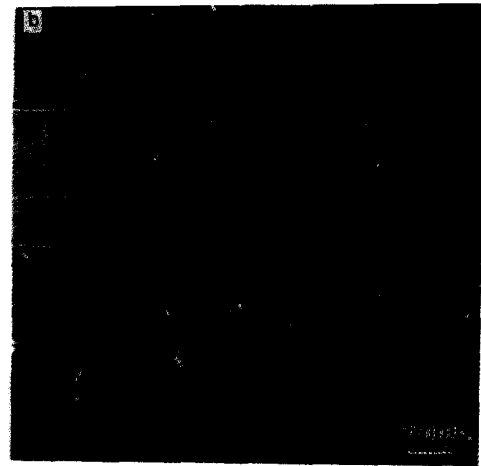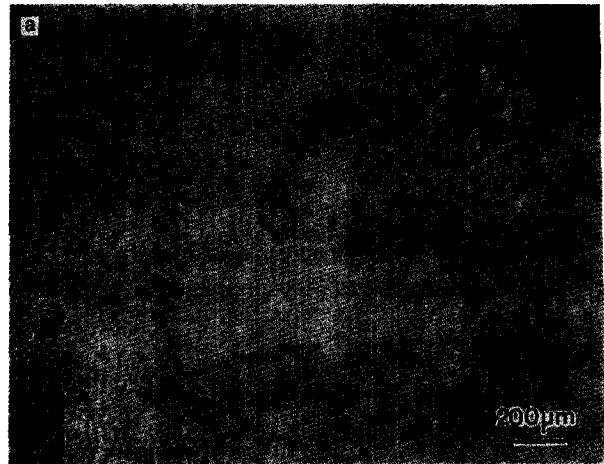Fig. 3. Shapes of the crept specimens of MA NiAl, tested at 110 MPa and 850℃ for 20 hrs.
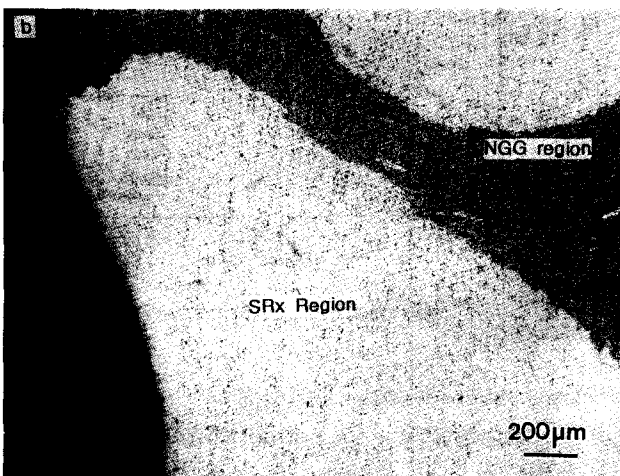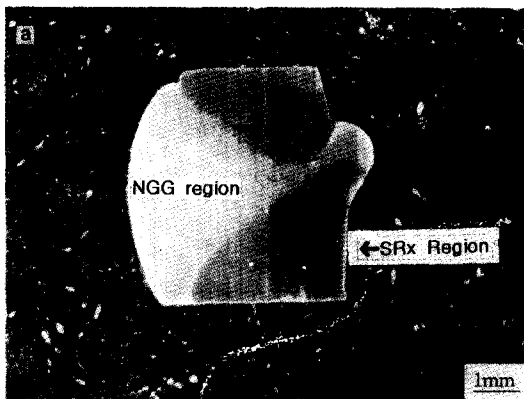

Fig. 4. Microstructure of crept specimen(SRx + NGG): (a) MP-4 photograph of longitudinal section, (b) optical micrograph of longitudinal section.

by 8mm long for SRx and partial SRx specimens, and 5mm diameter by 10mm long for NGG specimens. As can be seen, there is very little shape change in the SRx specimen, whereas the NGG specimen shows barreling and a significant decrease in length and increase in surface area which result in a lower effective stress and a

Fig. 5. Microstructure of crept specimen(SRx): (a) MP-4 photograph of longitudinal section, (b) optical micrograph of longitudinal section, single crystal.

lower apparent creep rate. The partially recrystallized specimen(SRx + NGG) shows NGG material in the center area being extruded from the sample.

Optical examination for the longitudinal cross section of the NGG + SRx specimen shows that the NGG portion is extruded perpendicular to the stress axis between two rigid secondary grains during the creep test, as shown in Fig. 4(a). This clearly indicates that the significant creep strain and creep rate in the specimen result from the material flow of the NGG area and highlights the difference in creep resistance between the SRx and NGG regions.

An optical micrograph for the locally bulged area is shown in Fig. 4(b). The brighter portion represents the SRx region and darker portion represents the NGG region. The alignment of grain morphology in NGG region represents the typical microstructures of the stress induced diffusional creep accommodated by grain boundary sliding[5,11]. On the other hand, the stringers of dispersoid appear to be stable without showing any indication of dispersoid coarsening or redistribution in the

Table 2. Steady State Creep Rates (sec^{-1}) for SRxed MA NiAl

	40MPa	110MPa	124.5MPa@
800℃		1.6×10⁻⁸ (0.55%)*	
850℃		6.6×10⁻⁸ (0.88%)* 4.0×10⁻⁸ (0.90%)	
900℃	6.59×10⁻⁹ (0.9%)	8.6×10⁻⁶ (1.43%)* 7.2×10⁻⁸ (1.7%)	4.57×10⁻⁷(31%)

Note: @ stress is a true stress converted from applied stress (180MPa)

　　　* denotes 2nd set of SRx specimens and the numbers in parenthesis indicate the total creep strain in 20 hrs.

SRx area.

SRx specimens for the creep test typically consist of less than 5 grains with each running the full length of the specimen, as presented in Fig. 5(a) and 5(b), and thus the creep properties of SRx specimens approximate the properties of <110> oriented single crystal DS NiAl.

Creep Mechanisms of SRxed MA NiAl.

The steady state creep rate ($\dot{\varepsilon}_s$) and the total creep strain for SRxed specimens are shown in Table 2.

The measured $\dot{\varepsilon}_s$ are shown to be slightly different depending on the batches of thermomechanical treatments, presumably due to morphological variations. NGG specimens were excluded in this discussion since the apparent decrease in creep rates due to large creep strain makes any comparison inappropriate. In the Table 2, the total creep strains are shown to be less than 2% over the whole temperature range below the stress of 110MPa, but 31% at an applied stress of 180MPa and 900℃.

In order to characterize the creep mechanisms, the activation energy and the creep exponent were calculated based on the creep data. The apparent activation energy for creep (Q_{app}) was obtained from an Arrhenius plot of ln $\dot{\varepsilon}_s$ versus 1/T at constant stress, as presented in Fig. 6;

$$Q_{app} = -R(\frac{\partial\, ln\, \dot{\varepsilon}_s}{\partial\,(1/T)})_{110MPa} = 177 \text{ kJ/mole}$$

The stress exponent (n) was also estimated from the plot of ln $\dot{\varepsilon}_s$ versus ln at constant temperature, as presented in Fig. 7;

$$n = (\frac{\partial\, ln\, \dot{\varepsilon}_s}{\partial\, ln\, \sigma})_{900c} = 3.05$$

The apparent activation energy for creep in SRx MA NiAl is almost the same as the activation energy (175 kJ/mole) in the as-extruded condition, but the apparent stress exponent for the SRx condition is higher than that (n=2) of as-extruded condition[12]. The activation
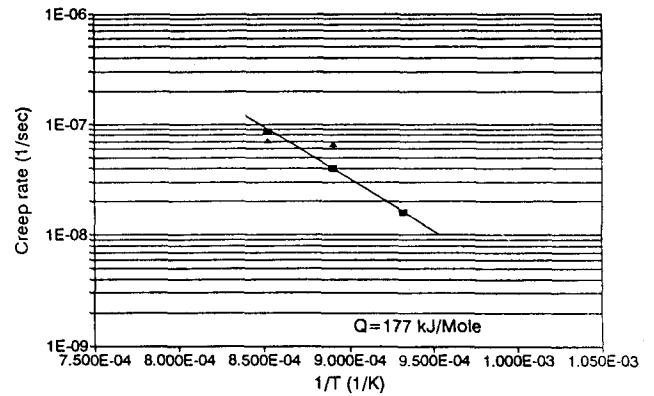

Fig. 6. Arrhenius representation of the temperature dependence of minimum creep rate(s^{-1}) at 110MPa in SRx MA NiAl.
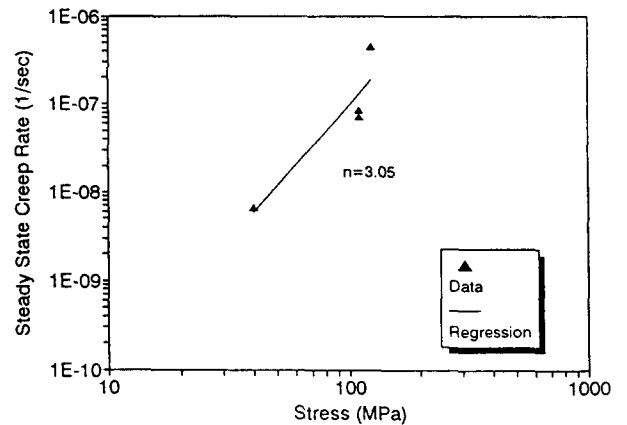

Fig. 7. Stress dependence of minimum creep rate($\dot{\varepsilon}_s$) of SRxed MA NiAl.

energy obtained in this study is in the range of the activation energy for the self diffusion of Ni(150~250 kJ/mole) in NiAl[13,14], indicating that the creep process is controlled by diffusion regardless of the dominant creep mechanisms[3,15].

Creep mechanisms are usually characterized using creep parameters such as activation energy, stress exponent and the range of test variables(T/T$_m$, σ/G), and the major rate controlling mechanisms can also be characterized pictorially in the form of maps[16]. Diffusional creep mechanism by stress assisted vacancy flow at low stresses(σ/G < 10^{-4}) and high temperatures such as

Table 3. Criteria for Classifying Dislocation Creep Behavior

	Class M(Type II)	Class A(Type I)
Controlling Mechanism	Climb	Viscous Glide
n	5	3
Q	Diffusion	Diffusion
Dilocation Structure	Subgrains	Homogeneous
Primary Creep	Normal Work Hardening	Inverted Yield Point

Nabarro-Herring or Coble creep, can be characterized by $n=1$ and very strong dependencies on grain size. At intermediate to high stress levels($10^{-2}<\sigma/G<10^{-4}$) and temperature range above $0.5T_m$, creep is believed to be controlled by the movement of diffusion controlled dislocations. This mechanism, so called dislocation climb controlled creep, is characterized by $n=5$ and independencies on grain size. At high stresses($\sigma/G>10^{-2}$), dislocation glide, which involves dislocation moving along slip planes and overcoming barriers by thermal activation, is believed to be rate controlling. Another high temperature mechanism involves grain boundary sliding, which does not represent an independent mechanism and thus be accommodated by other deformation modes[1]. In this classification, both diffusion controlled dislocation climb mechanism and viscous glide controlled mechanism are frequently refered to the dislocation creep in many cases[3,16,17].

As recently summarized by Nathal[17], dislocation creep for single phase metals and alloys can be classified as either of two main types, known as class M, or pure metal type, and class A, or alloy type, as presented in Table 3. Class M creep is characterized by glide being much faster than climb, and thus creep is controlled by the rate of climb past substructural obstacles. Class A creep is often so called viscous glide controlled creep, since the glide of dislocations is restricted by solute atoms or perhaps by a high lattice friction stress due to long range order and this reduced glide mobility is the limiting creep process. However, these categories represent limiting conditions, and many materials exhibit an intermediate behavior comprised of a mixture of the defining traits.

Compressive creep properties of single phase NiAl, both in polycrystalline and single crystal forms, were investigated by many authors[18,19,20] and summarized by Nathal[17]. Since the best choices for Q and n were shown to be about 310 kJ/mol and 6, respectively, it was considered that dislocation creep was responsible for high temperature creep (700~1000℃) of single phase NiAl, and that the rate of the process was controlled by dislocation climb.

As far as the as-consolidated MA NiAl concerned, the activation energies for creep (175~225 kJ/mol) were shown to be within the range of activation energies determined in diffusion experiments and stress exponent(2~3.8) were shown to be significantly lower than those for single phase NiAl[12]. Although the stress exponent seems to fall into the viscous glide controlled mechanism in Table 3, the creep for MA NiAl was speculated to be controlled rather by dislocation climb due to the following reasons:

a) Creep was investigated in the stress range between $5\times10^{-4}G$ and $5\times10^{-3}G$ away from both the stress range of diffusional creep($<10^{-4}G$) and the range of viscous glide($>10^{-2}G$).

b) Test temperature range were between 0.5 and 0.6 T_m away from the range of diffusional flow(above 0.6 T_m).

c) MA NiAl exhibit the threshold stress(about 20MPa) behavior, which are believed due to dislocation-dispersoid interaction.

Therefore, taking into consideration the test range in the present study($0.56\leq T/TM\leq0.61$ and $4\times10^{-4}\leq\sigma/G\leq3\times10^{-3}$), the measured value of stress exponent(n $=3.05$), the activation energy for creep($Q_{app}=177$kJ/mol), the occurrence of the threshold stress and the normal work hardening shape of primary creep curve in Fig. 2, it can be considered that the creep in SRxed MA NiAl is controlled rather by dislocation climb than viscous glide.

Creep of DS materials is commonly characterized by high values of apparent activation energy for creep, and abnormally high values of stress exponent(n~40), and the existence of a threshold stress(σ_{th}) below which no measurable creep rate can be detected[3,21,22]. Lund and Nix suggested that the abnormally high values of Q_{app} were attributable to the temperature dependence of the elastic modulus and the abnormally high values of n in DS materials[21]. The abnormally high n value in DS alloys arises from the presence of a threshold stress which is believed to originate from the resistance to dislocation motion by particles[3,4]. However, SRxed MA NiAl exhibits a normal apparent activation energy for

creep and apparent stress exponent. This is in part due to the relatively insensitive temperature dependence of the elastic modulus in NiAl[23], and the low threshold stress value observed in as-consolidated MA NiAl[12].

In order to rationalize the elastic modulus effect on Q_{app}, the true activation energy(Q_c) for creep was estimated using the elastic modulus compensated creep equation proposed by Shelby[24]. The equation is given by;

$$\dot{\varepsilon}_s = A^- (\frac{\sigma}{E(T)})^m exp(-\frac{Q_c}{RT})$$

Since the creep rate of many ODS alloys is determined by an effective stress$(\sigma - \sigma_{th})^{3,22}$, the normalized creep equation with respect to the effective stress is generally expressed by ;

$$\dot{\varepsilon}_s = A_o(\frac{\sigma - \sigma_{th}}{E(T)})^n {}_o exp(-\frac{Q_c}{RT})$$

where A_o is a structural dependent constant and n_o is the true stress exponent, Q_c is the true activation energy and other parameters have their usual meaning. Comparing the equation with the normal creep equation, n_o can be rationalized with respect to the apparent n;

$$n_o = n\frac{\sigma - \sigma_{th}}{\sigma} = n[1 - (\frac{\sigma - \sigma_{th}}{\sigma})]$$

As can be seen, the apparent n value will increase for any finite value of σ_{th}, and the larger the σ_{th} the larger the n value will be for a given σ. From the equations, Q_c can be derived by;

$$Q_c = -R[\frac{\partial ln \dot{\varepsilon}_s}{\partial(1/T)}]_\sigma - nR\frac{dlnE(T)}{dln(1/T)} = Q_{app} + nR\frac{T^2}{E}\frac{\partial E}{\partial T}$$

Assuming no significant differences in elastic modulus between SRx and as-extruded condition, an elastic modulus equation which was experimentally determined for <110> oriented single crystal NiAl[24] was applied in this calculation ;

E(T) = 195.055 − 0.0349T(GPa), where T is in K.

Based on this equation, the E(900℃) and E/ T(900 ℃) were found to be 154.1GPa and −0.0349 GPa/K, respectively. Using n=3.05 and Q_{app}=177kJ/mole, the true activation energy was estimated to be 169.1 kJ/ mole. Thus the Q_{app} measured in SRxed MA NiAl is very similar to the true value because of the relatively insensitive temperature dependence of the elastic modu-

lus. A similar result was shown in a previous creep study for as-extruded MA NiAl in which Q_{app} and Q_c are 175 and 174.2 kJ/mole, respectively[12].

As discussed earlier, no apparent grain size effect is expected in dislocation creep[4,11,17], however, minimum creep rates are shown to be very sensitive to grain size when compared to the previous creep results on as-extruded material[12]. The creep rates appear to be decreased about two orders of magnitude with increasing grain size in the SRxed condition. This suggests that the grain boundary sliding mechanism[5,11], which is believed to be accommodated by one of the dislocation creep mechanism in the as-extruded condition, is suppressed by a reduction in the numbers of grain boundaries with an imposed shear stress in the SRx condition resulting in lower creep rates. In addition to the grain size effect, the inherently fine dispersoid size in the SRxed condition is believed to play an important role in this creep, since dispersoid coarsening is known to lead to an increased creep rate despite an increase in grain size in the NGG condition.

Effect of Microstructure on Creep.

Compressive creep properties of SRxed MA NiAl at 900℃[12] are compared with the creep data for the as-consolidated MA NiAl tested at 900℃ and published creep data for NiAl tested at 927℃(1200K)[25~27], as shown in Fig. 8. Creep properties of MA NiAl were shown to be enhanced by mechanical alloying process in comparison with their cast counter part or other DS NiAl produced by Rapid Solidification Technology. SRx specimens having a coarse grain structure with fine dispersoid were shown to exhibit significantly improved creep properties. The grain aspect ratio in the SRxed specimens was about 5 with full grain length parallel to the stress axis, whereas all of the other materials were equiaxed. It has been shown that the high temperature strength and the threshold stress generally increase with increasing GAR in DS materials[28,29] due to the minimization of grain boundary sliding by reduction of the number of grain boundaries with an imposed shear stress. In addition, high GAR morphology can reduce cavity formation and growth as proposed by Arzt and Singer, leading to reduction in creep rates[7]. Arzt and Singer suggested that cavity growth on transverse boundaries (in tension) produces incompatibilities between neighboring grains but it can be eliminated by local grain boundary sliding in the longitudinal direction[7]. However, such an improvement in creep properties by minimizing cavitation in high GAR is not expected in compression mode[27,30].
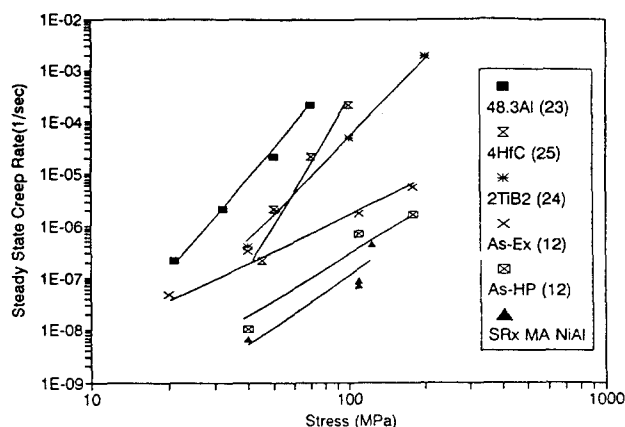
Fig. 8. Comparison of creep properties of SRxed MA NiAl with other DS NiAl: as-extruded(As-EX), as hot pressed(As-HP) and SRx MA NiAl were teted at 900℃, and others were at 927℃.

It is also reported that the creep rates will be significantly different depending on testing modes especially in small sized and equiaxed specimens[30]. Timmins and Arzt have shown that creep parallel to the longitudinal grain direction of MA6000(high GAR structure) in tension is similar to that in compression whereas transverse creep in tension is considerably worse in comparison to the compression mode in which cavitation is almost completely suppressed[30]. In other words, an increase in the number of transverse grain boundaries (as in small grain size) resulted in considerable creep rate enhancement in tension, while such a change was not observed in compression. Although the cavitation mechanism is not expected in compression creep mode, the minimization of grain boundary sliding by reduction of grain boundaries under the shear stress can still be of significance in compression creep.

4. Conclusions

1) Enhanced dispersoid coarsening during normal grain growth led to poor creep properties similar to single phase NiAl, despite an increase in grain size. On the other hand, pronounced grain coarsening and high GAR combined with fine dispersoid size produced by SRx resulted in improved creep resistance in comparison to the creep in both the as-extruded condition and the normal grain growth condition.

2) The apparent activation energy and stress exponent for creep in SRxed MA NiAl were found to be 177 kJ/mole and 3.05, respectively. Taking into consideration the test range in the present study($0.56 \leq T/T_M \leq 0.61$ and $4 \times 10^{-4} \leq \sigma/G \leq 3 \times 10^{-3}$), the measured value of stress exponent, the activation energy for creep, the occurrence of the threshold stress and the normal work

hardening shape of primary creep curve, it can be considered that the creep in SRxed MA NiAl is controlled rather by dislocation climb than viscous glide.

3) Although the creep in SRxed MA NiAl can be considered to be controlled by one of the dislocation creep mechanisms which are generally grain size independent, strong grain size dependency has been shown. The minimum creep rate in SRx material was decreased one or two orders of magnitude in comparison to the creep in the as-extruded condition. Improved creep resistance of SRxed MA NiAl may be postulated to result from a contribution from grain boundary sliding to the creep rate of these materials. In addition to the grain size effect, the inherently fine dispersoid size in the SRxed condition is believed to play an important role in this creep, since dispersoid coarsening is known to lead to an increased creep rate despite an increase in grain size in the NGG condition.

4) Secondary recrystallization of dispersion strengthened intermetallics offers a potential processing route for optimization of the high temperature mechanical properties.

References

1. R. Darolia, J. Met., **43**(3), 44, (1991).
2. G. Sauthoff, Proc. of the German Society of Mat. Sci. Conf. on Microstructure and Mechanical Properties of Materials, Bad Nauheim, 363, (1991).
3. C. M. Sellars and R. A. Petkovic-Luton, Mat. Sci. Eng., **46**, 75, (1980).
4. V. C. Nardone, D. E. Matejcjyk and J. K. Tien, Acta Metall., **32**(9), 1509, (1984).
5. R. Raj and M. F. Ashby, Metall. Trans., **2**, 1113, (1971).
6. K. Mino, Y. G. Nakagawa and A. Ohtomo, Metall. Trans., A, **58**(5), 717, (1987).
7. E. Arzt and R. F. Singer, Proc. of 5th Int. Symp. on Superalloys, TMS of AIME, 367, (1984).
8. S. C. Ur, G. T. Higgins and P. Nash, Scripta Metall., **34**(1), 53, (1996).
9. M. Dollar, S.Dymek, S. J. Hwang and P. Nash, Metall. Trans, **24A**, p.1993, (1993)
10. J. D. Whittenberger, R. K. Viswanadham, S. K. Mannan and K. S. Kumar, J. of Mater. Res., **4**(5), 1164, (1989).
11. R. W. Herzberg, Deformation and Fracture Mechanism of Engineering Materials, 3rd ed., John-Wiley and Sons, (1989).
12. S. J. Suh, Mater. Sci. & Eng., **A192/193**, 691, (1995).

13. A. Lutze-Birk and H. Jacobi, Scripta Metall., **9**, 761, (1975).
14. S. Shankar and L. L. Seigle, Metall. Trans., **9A**, 1467, (1978).
16. M. F. Ashby, Acta Metall., **20**, 87, (1972).
17. M. V. Nathal, Ordered Intermetallics, C. T. Liu, ed., Kluwer Academic Publshers, 541, (1992).
18. R. R. Vandervoort, A. K. Mukherjee and J. E. Dorn, Trans. ASM, **59**, 931, (1966).
19. M. Rudy and G. Sauthoff, High Temperature Ordered Intermetallic Alloys, eds., C. C. Kock, C. T. Liu and N. S. Stoloff, **39**, 327, (1985).
20. J. D. Whittenberger, J. Mater. Sci., **23**, 327, (1988).
21. R. W. Lund and W. D. Nix, Metall. Trans., **6A**, 1329, (1975).

22. J. D. Whittenberger, Metall. Trans., **8A**, 1155, (1977).
23. D. B. Miracle, Acta Metall., **41**(3), 649, (1993).
24. R. J. Wasilewski, Metall. Trans., **236**, 455, (1966).
25. J. D. Whittenberger, J. Mater. Sci., **22**, 395, (1987).
26. J. D. Whittenberger, R. Ray, S. C. Jha and S. Draper, Mater. Sci and Eng., **A138**, 83, (1991).
27. J. D. Whittenberger, R. Ray and S. C. Jha, Mater. Sci and Eng., **A151**, 137, (1992).
28. B. A. Wilcox and A. H. Clauer, Acta Metall., **20**, 743, (1972).
29. R. L. Cairns, L. R. Curwik and J. S. Benjamin, Metall. Trans., **6A**, 179, (1974).
30. R. Timmins and E. Arzt, Structural Application of MA, F. H. Froes, eds., ASM, 67, (1991).